REFERENCES

1. Watanabe T, Itabashi M, Shimada Y, et al. Japanese Society for Cancer of the Colon and Rectum (JSCCR) guidelines 2010 for the treatment of colorectal cancer. Int J Clin Oncol 2012; 17:1–29.
2. Colucci G, Gebbia V, Paoletti G, et al. Phase III randomized trial of FOLFIRI versus FOLFOX4 in the treatment of advanced colorectal cancer: a multicenter study of the Gruppo Oncologico Dell'Italia Meridionale. J Clin Oncol 2005; 23:4866–4875.
3. Goldberg RM, Sargent DJ, Morton RF, et al. A randomized controlled trial of fluorouracil plus leucovorin, irinotecan, and oxaliplatin combinations in patients with previously untreated metastatic colorectal cancer. J Clin Oncol 2004; 22:23–30.
4. Tournigand C, Andre T, Achille E, et al. FOLFIRI followed by FOLFOX6 or the reverse sequence in advanced colorectal cancer: a randomized GERCOR study. J Clin Oncol 2004; 22:229–237.
5. Shitara K, Matsuo K, Yokota T, et al. Prognostic factors for metastatic colorectal cancer patients undergoing irinotecan-based second-line chemotherapy. Gastrointest Cancer Res 2011; 4:168–172.
6. Huppert P, Wenzel T, Wietholtz H. Transcatheter arterial chemoembolization (TACE) of colorectal cancer liver metastases by irinotecan-eluting microspheres in a salvage patient population. Cardiovasc Intervent Radiol 2014; 37:154–164.
7. Martin RC II, Scoggins CR, Tomalty D, et al. Irinotecan drug-eluting beads in the treatment of chemo-naive unresectable colorectal liver metastasis with concomitant systemic fluorouracil and oxaliplatin: results of pharmacokinetics and phase I trial. J Gastrointest Surg 2012; 16:1531–1538.
8. Seki A, Hori S. Transcatheter arterial chemoembolization with docetaxel-loaded microspheres controls heavily pretreated unresectable liver metastases from colorectal cancer: a case study. Int J Clin Oncol 2011; 16: 613–616.
9. Eichler K, Zangos S, Mack MG, et al. First human study in treatment of unresectable liver metastases from colorectal cancer with irinotecan-loaded beads (DEBIRI). Int J Oncol 2012; 41:1213–1220.
10. Aliberti C, Fiorentini G, Muzzio PC, et al. Trans-arterial chemoembolization of metastatic colorectal carcinoma to the liver adopting DC Bead(R), drug-eluting bead loaded with irinotecan: results of a phase II clinical study. Anticancer Res 2011; 31:4581–4587.
11. Fiorentini G, Aliberti C, Tilli M, et al. Intra-arterial infusion of irinotecan-loaded drug-eluting beads (DEBIRI) versus intravenous therapy (FOLFIRI) for hepatic metastases from colorectal cancer: final results of a phase III study. Anticancer Res 2012; 32:1387–1395.
12. Jordan O, Denys A, De Baere T, Boulens N, Doelker E. Comparative study of chemoembolization loadable beads: in vitro drug release and physical properties of DC Bead and Hepasphere loaded with doxorubicin and irinotecan. J Vasc Interv Radiol 2010; 21:1084–1090.
13. Maeda N, Osuga K, Tanaka K, et al. In vitro characterization of drug-eluting Hepasphere designed for chemoembolization. Presented at the annual meeting of Cardiovascular and Interventional Radiological Society of Europe; September 13, 2014; Glasgow, UK.
14. de Luis E, Bilbao JI, de Ciercoles JA, Martinez-Cuesta A, de Martino Rodriguez A, Lozano MD. In vivo evaluation of a new embolic spherical particle (HepaSphere) in a kidney animal model. Cardiovasc Interv Radiol 2008; 31:367–376.
15. Jiaqi Y, Hori S, Minamitani K, et al. A new embolic material: super absorbent polymer (SAP) microsphere and its embolic effects. Nippon Acta Radiol 1996; 56:19–24.
16. Seo TS, Oh JH, Lee DH, Ko YT, Yoon Y. Radiologic anatomy of the rabbit liver on hepatic venography, arteriography, portography, and cholangiography. Invest Radiol 2001; 36:186–192.
17. Kim TW, Innocenti F. Insights, challenges, and future directions in irinogenetics. Ther Drug Monit 2007; 29:265–270.
18. Smith NF, Figg WD, Sparreboom A. Pharmacogenetics of irinotecan metabolism and transport: an update. Toxicol In Vitro 2006; 20:163–175.
19. Rao PP, Pascale F, Seck A, et al. Irinotecan loaded in eluting beads: preclinical assessment in a rabbit VX2 liver tumor model. Cardiovasc Intervent Radiol 2012; 35:1448–1459.
20. Tanaka T, Nishiofuku H, Hukuoka Y, et al. Pharmacokinetics and antitumor efficacy of chemoembolization using 40 μm irinotecan-loaded microspheres in a rabbit liver tumor model. J Vasc Interv Radiol 2014; 25: 1037–1044.
21. Guichard S, Terret C, Hennebelle I, et al. CPT-11 converting carboxylesterase and topoisomerase activities in tumour and normal colon and liver tissues. Br J Cancer 1999; 80:364–370.
22. Hong K, Khwaja A, Liapi E, Torbenson MS, Georgiades CS, Geschwind JF. New intra-arterial drug delivery system for the treatment of liver cancer: preclinical assessment in a rabbit model of liver cancer. Clin Cancer Res 2006; 12:2563–2567.
23. Maeda N, Osuga K, Shimazu K, et al. In vivo evaluation of cisplatin-loaded superabsorbent polymer microspheres for use in chemoembolization of VX2 liver tumors. J Vasc Interv Radiol 2012; 23:397–404.
24. Parvinian A, Casadaban LC, Gaba RC. Development, growth, propagation, and angiographic utilization of the rabbit VX2 model of liver cancer: a pictorial primer and "how to" guide. Diagn Intervent Radiol 2014; 20: 335–340.
25. Richardson AJ, Laurence JM, Lam VW. Transarterial chemoembolization with irinotecan beads in the treatment of colorectal liver metastases: systematic review. J Vasc Interv Radiol 2013; 24:1209–1217.

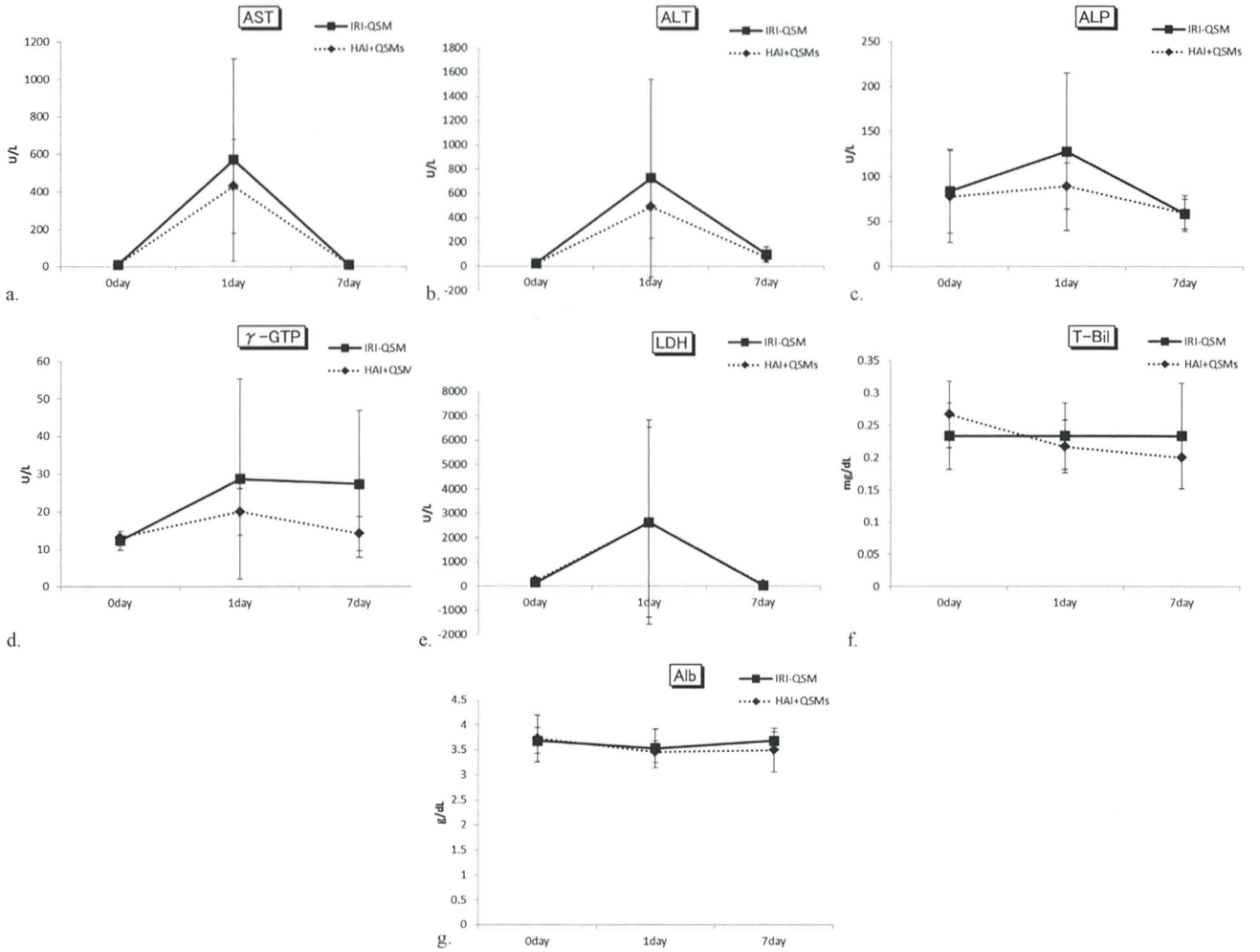

Figure E1. Serum chemistry at 7 days after the start of treatment. There was no statistically significant difference in any parameter and at any time point between the two groups ($P > .05$). The peak values of liver enzymes (**a**, aspartate aminotransferase; **b**, alanine aminotransferase; **c**, alkaline phosphatase, and **d**, γ-glutamyl peptidase) were higher in the irinotecan-loaded QuadraSphere (IRI-QSM) group, but the difference was not significant ($P > .05$). Lactate hydrogenase **(e)**, albumin **(f)**, and total bilirubin **(g)** levels remained unchanged after treatment.

Embolic Effects of Transcatheter Mesenteric Arterial Embolization with Microspheres on the Small Bowel in a Dog Model

Kentaro Kishimoto, MD, Keigo Osuga, MD, PhD, Noboru Maeda, MD, PhD, Yoshiyuki Higashi, DVM, Akiyoshi Hayashi, DVM, PhD, Yumiko Hori, MD, Masahisa Nakamura, MD, Fumihito Ohashi, DVM, PhD, Eiichi Morii, MD, PhD, and Noriyuki Tomiyama, MD, PhD

ABSTRACT

Purpose: To determine the arterial distribution and ischemic effects of various particle sizes after transcatheter embolization of the small bowel in a dog model.

Materials and Methods: In 10 dogs, selective microsphere embolization was performed in six branches of the superior mesenteric artery. Microspheres were allocated into three size ranges (100–300 μm, 300–500 μm, and 500–700 μm) and four volume concentrations (0.625%, 1.25%, 2.5%, and 5%). For each size and volume concentration, embolization was performed of five branches at the origin of the last arcade. The distribution of microspheres and the range of ischemic changes of mucosa were evaluated histologically. Angiograms were categorized into two groups: group A, only the vasa recta nonopacified; group B, the last arcade or more proximal branches nonopacified.

Results: Microspheres sized 100–300 μm penetrated into intramural arteries and 500–700 μm microspheres mainly blocked arteries in the mesentery. There was a significant difference among three sizes in terms of the locations within the vasculature ($P < .0001$). The larger volume and the smaller size resulted in more ischemia. The range of ischemic changes among three sizes and among four volume concentrations was significantly different ($P = .004$ and $P < .0001$, respectively). The range of ischemic changes with 500–700 μm microspheres in group B was significantly greater than in group A (0% in group A vs 83% in group B, $P = .001$).

Conclusions: In a dog model, embolization of the small bowel limited to the vasa recta with the use if 500–700 μm microspheres reduced the range of ischemic changes.

ABBREVIATIONS

ANOVA = analysis of variance, LGI = lower gastrointestinal, NBCA = *N*-butyl cyanoacrylate

Lower gastrointestinal (LGI) arterial bleeding is defined as hemorrhage below the ligament of Treitz and includes jejunal, ileal, colonic, and rectal bleeding (1,2). LGI bleeding is often difficult to manage by endoscopic therapy, and therapeutic options in the event of endoscopic failure include surgery and transcatheter therapy (3). Microcoils have been the embolic agent of choice for LGI bleeding because they are highly visible under fluoroscopy (1,3–5). However, in clinical practice with current low-profile microcatheter technology, there are situations where the microcatheter cannot be advanced into the bleeding site of the vessel. In these cases, alternative embolic agents have to be considered, including particle and liquid agents.

Microspheres are calibrated spherical particles with diameters in the micrometer range (6–8). Because of their uniform, spherical shape and soft, smooth surface, they show a more distal distribution than nonspherical particles, and the occlusion level of the arteries can be predicted according to the particle size (9–11). Because

From the Departments of Diagnostic and Interventional Radiology (K.K., K.O., N.M., M.N., N.T.) and Pathology (Y.Ho., E.M.), Osaka University Graduate School of Medicine, 2-2 Yamadaoka Suita, Osaka 565-0871, Japan; and Laboratory of Veterinary Surgery (Y.Hi., A.H., F.O.), Department of Graduate School of Life and Environmental Sciences, Osaka Prefecture University, Osaka, Japan. Received March 14, 2014; final revision received June 18, 2014; accepted June 23, 2014. **Address correspondence to** K.K.; E-mail: k-kishimoto@radiol.med.osaka-u.ac.jp

K.O. was supported by JSPS KAKENHI Grant #23591819. None of the other authors have identified a conflict of interest.

J Vasc Interv Radiol 2014; 25:1767–1773

http://dx.doi.org/10.1016/j.jvir.2014.06.020

the vascular resistance of a bleeding vessel is lower than that of a normal vessel, microspheres can move preferentially to the bleeding site with the blood flow (12), and the use of a small volume of microspheres with proper particle size might be enough to stop bleeding. Transcatheter arterial embolization with microspheres for LGI bleeding was reported in a retrospective clinical study (13). However, the distribution of microspheres to the normal intestine around the bleeding site is inescapable, and ischemic change can resulted. It is important to know what level of artery within the mesentery and intestine is occluded and the extent of ischemic damage caused by transcatheter arterial embolization with varying particle sizes. The purpose of this study was to determine the arterial distribution and ischemic effects of varying particle sizes after transcatheter arterial embolization of the small bowel in a dog model.

MATERIALS AND METHODS

Study Design

This study was approved by the animal care committee of our institution. Subjects for this experiment included 10 healthy male beagle dogs (weight, 10–15 kg). Selective embolization of six isolated target branches of the superior mesenteric artery was performed in each dog; 60 branches in all received embolization.

Embolic Materials

In this study, calibrated tris-acryl gelatin microspheres (Embospheres; Merit Medical Systems, South Jordan, Utah) of three size ranges (100–300 μm, 300–500 μm, and 500–700 μm) were investigated. Microspheres were prepared in 1-mL suspensions with volume concentrations of 0.625%, 1.25%, 2.5%, and 5%. All suspensions were obtained with the same iodine concentration (150 mgI/mL).

Preparation of Experimental Animals

Anesthesia was induced via subcutaneous injection of 50 μg/kg of atropine sulfate (Mitsubishi Tanabe Pharma Corporation, Osaka, Japan) and 6–8 mg/kg/h of propofol (Mylan, Inc, Tokyo, Japan) and was maintained with inhalation isoflurane (Intervet, Tokyo, Japan). The dogs were positioned supine, and their legs were tethered. The upper abdominal and right inguinal area was sterilized, and laparotomy was performed. All procedures were performed aseptically.

Selective Embolization

A 4-F short introducer sheath (Medikit Co, Ltd, Tokyo, Japan) was inserted into the right femoral artery by means of the Seldinger technique. The superior mesenteric artery was selected with a 4-F Cobra catheter (Cook Medical, Tokyo, Japan). A 1.9-F microcatheter (Carnelian PIXIE; Tokai Medical Products, Kasugai, Japan) was advanced into the origin of the last arcade of small intestines including ileum and jejunum using a 0.016-inch guide wire (Meister; Asahi Intecc, Aichi Co, Ltd, Japan). The injection of microspheres was performed slowly (< 0.5 mL/min) with fluoroscopic control using a 1.0-mL syringe. After injection of a predetermined size or quantity of microspheres, the microcatheter was purged with a volume of 3 mL of saline. For each size and volume concentration of microspheres, selective embolization of five separate arcades in the different dogs was performed. The microcatheter position was identified under direct vision, and the mesentery in the segment that received embolization was marked with string. As a rule, embolization of the neighboring two arcades was avoided.

Angiographic Evaluation

Digital subtraction angiograms were obtained before and 5 minutes after embolization for each segment by manual injection of contrast medium. To search whether the angiographic endpoint is useful for prediction of ischemic change of the small bowel, segments were divided into two groups on the basis of angiographic findings after embolization as follows: in group A, only the vasa recta nonopacified; in group B, the last arcade or more proximal branches nonopacified. The relationship between the range of ischemic changes and angiographic findings was analyzed.

Sacrifice and Histologic Evaluation

The dogs were killed with an intravenous injection of pentobarbital sodium 48 hours after transcatheter arterial embolization for investigation of ischemic changes in the small bowel. Necropsy was performed on each dog, and the small bowel was removed. The resected segments of the small bowel were fixed in a 10% neutral formaldehyde buffer for histologic evaluation. From each segment, two adjacent sections were taken from areas perceived to be the most discolored or abnormal. If there were no such changes, two sections were taken from the center of the segment that received embolization. The sections were stained with hematoxylin-eosin to identify microspheres in the vasculature and to investigate for damage to the small bowel. Histologic evaluation was performed by an experienced pathologist using microscopic examination. To evaluate the distribution of microspheres, locations were categorized into the mesenteric arteries apart from intestine, extramural arteries along the intestinal wall, and intramural arteries (Fig 1). The number of microspheres in each location was counted. To evaluate ischemic mucosal damage, the proportions of cross-sectional area with ischemic changes to the entire circumferential area were evaluated histologically with a percentage scale. Ischemic changes

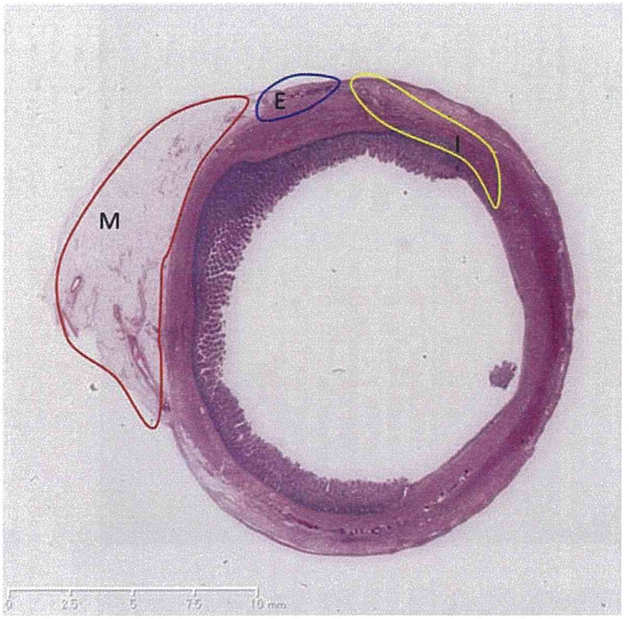

Figure 1. The arteries of the mesentery and the small bowel are divided into three locations. M = mesentery; E = extramural; I = intramural.

were determined if there were pathologic findings, such as congestion, edema, hemorrhage, and necrosis. Of the two sections, the one with the higher proportion of ischemic change represented each segment that received embolization.

Statistical Analysis

The χ^2 test was performed to compare the location of occlusion among three different sizes of microspheres. The two-factor factorial analysis of variance (ANOVA) was applied to assess the statistical significance of the difference in the range of ischemic changes of the small bowel between microspheres of three different sizes and between four volume concentrations of microspheres. The Mann-Whitney *U* test was used to compare continuous variables of the range of ischemic changes between group A and group B for each size.

RESULTS

Selective embolization was achieved in all segments. All dogs were alive until sacrifice. All segments were located in the small bowel. In one dog, ascites was seen, and perforation of the small bowel was found in one segment that received embolization with 100–300 μm microspheres (volume concentration 5%).

Microspheres Distribution in the Vasculature

Numbers and percentages of microspheres detected in each location are listed in Table 1. Microspheres sized 100–300 μm were distributed in all locations (Fig 2a–d), and 35% of 100–300 μm microspheres were detected within the intramural arteries. Of 500–700 μm microspheres, 87% were located in the mesentery (Fig 3a–d). The smaller microspheres blocked vessels more distally than the larger microspheres. There was a significant difference between three size ranges of microspheres in terms of their locations within the vasculature ($P < .0001$, χ^2) (Table 1).

Table 1. Percentage of Microspheres Detected in the Different Locations

Location	100–300 μm	300–500 μm	500–700 μm
Mesentery	36% (n = 110)	45% (n = 47)	87% (n = 20)
Extramural	29% (n = 89)	35% (n = 37)	4% (n = 1)
Intramural	35% (n = 109)	20% (n = 21)	9% (n = 2)
Total	100% (n = 308)	100% (n = 105)	100% (n = 23)
P value (χ^2)	< .0001		

Ischemic Change

Figure 4 shows the relationship between the proportion of the ischemic changes of the mucosal layer and volume concentration of microspheres. There was no significant interaction of ischemic effects between size and volume concentration of microspheres ($P = .71$, two-factor factorial ANOVA). Larger volume of microspheres resulted in more ischemic changes, and smaller size of microspheres resulted in more ischemic changes. There was a significant difference in ischemic changes when comparing among the three size ranges ($P = .004$, two-factor factorial ANOVA) and when comparing among the four volume concentrations ($P < .0001$, two-factor factorial ANOVA).

Angiographic Findings

The relationship between the proportions of ischemic changes and the angiographic findings are listed in Table 2. In group B, the mean proportions of the ischemic changes were 90% for 100–300 μm, 75% for 300"500 μm, and 83% for 500–700 μm. A broader range of ischemic changes was observed in group B than in group A for all three size ranges of microspheres. The differences in the proportions of ischemic changes between group A and Group B were not statistically significant for 100–300 μm or 300–500 μm microspheres ($P = .29$ and $P = .0502$, respectively), whereas the difference was statistically significant for 500–700 μm microspheres (P = .001).

DISCUSSION

Transcatheter arterial embolization for LGI bleeding aims to achieve hemostasis, but the intestinal damage should be minimized. Historically, transcatheter arterial embolization has been performed from more proximal

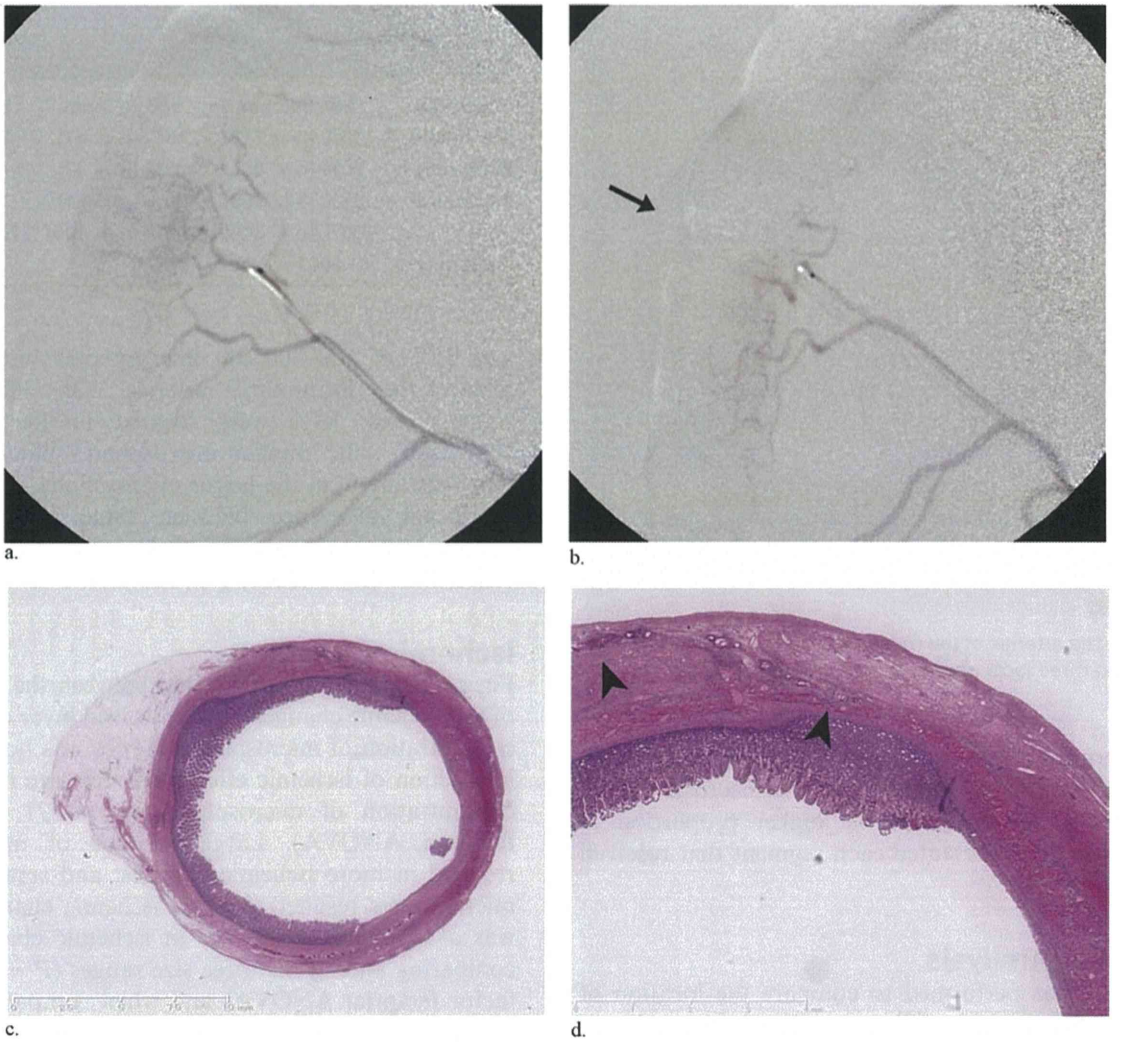

Figure 2. Selective superior mesenteric arteriogram before embolization shows vasa recta and mucosal blush **(a)**. After embolization with 100–300 μm microspheres (volume concentration 5%), the vasa recta and the corresponding arcade are occluded (arrow) **(b)**. In the histologic axial-cut specimen (hematoxylin-eosin stain), the entire mucosal layer and the antimesenteric side of the submucosal layer and muscle layer show congestion, edema, and hemorrhage. Stripping of endothelial cells is observed on the antimesenteric side **(c)**. Numerous microspheres are observed from extramural to intramural arteries (arrowheads) **(d)**. (Available in color online at *www.jvir.org*.)

arteries rather than targeting the actual site of bleeding to decrease the arterial inflow. However, the goal of transcatheter arterial embolization has shifted toward direct mechanical blockage of the specific bleeding vessel.

Microcoils are mainly used for LGI bleeding because they have good radiopacity and allow controlled deployment at the bleeding site (1). However, selective microcatheter insertion may be difficult in very tortuous or narrowed atherosclerotic arteries, and the use of particles such as polyvinyl alcohol and liquid embolic agents such as *N*-butyl cyanoacrylate (NBCA) can be an alternative option. Kusano et al (14) reported that polyvinyl alcohol particles $\geq$ 420 μm were safely used in experimental and clinical studies. However, concern remains about unexpected ischemic intestinal damage because polyvinyl alcohol particles tend to aggregate in proximal vessels owing to inhomogeneous sizes, and occlusion levels are unpredictable. Tiny fragments can also be contaminated and penetrate to the capillary level (11). In contrast, calibrated microspheres are homogeneous in size, and the occlusion level is predictable according to the particle size (6,10,15,16). Similar to previous experimental studies in the uterus and kidney (6,10,15,16), a significant correlation between the locations and the size ranges of microspheres was observed in the intestinal wall in the present study.

The combination of NBCA and ethiodized oil (Lipiodol; Laboratoire Guerbet, Villepinte, France) has also been evaluated as an embolic agent for intestinal artery embolization in experimental and clinical studies. In studies by Jae et al (17) and Ikoma et al (18), embolization using NBCA and ethiodized oil of three or fewer vasa recta was tolerable in the small bowel (17) and in the colon (18). Jae et al (17) reported that

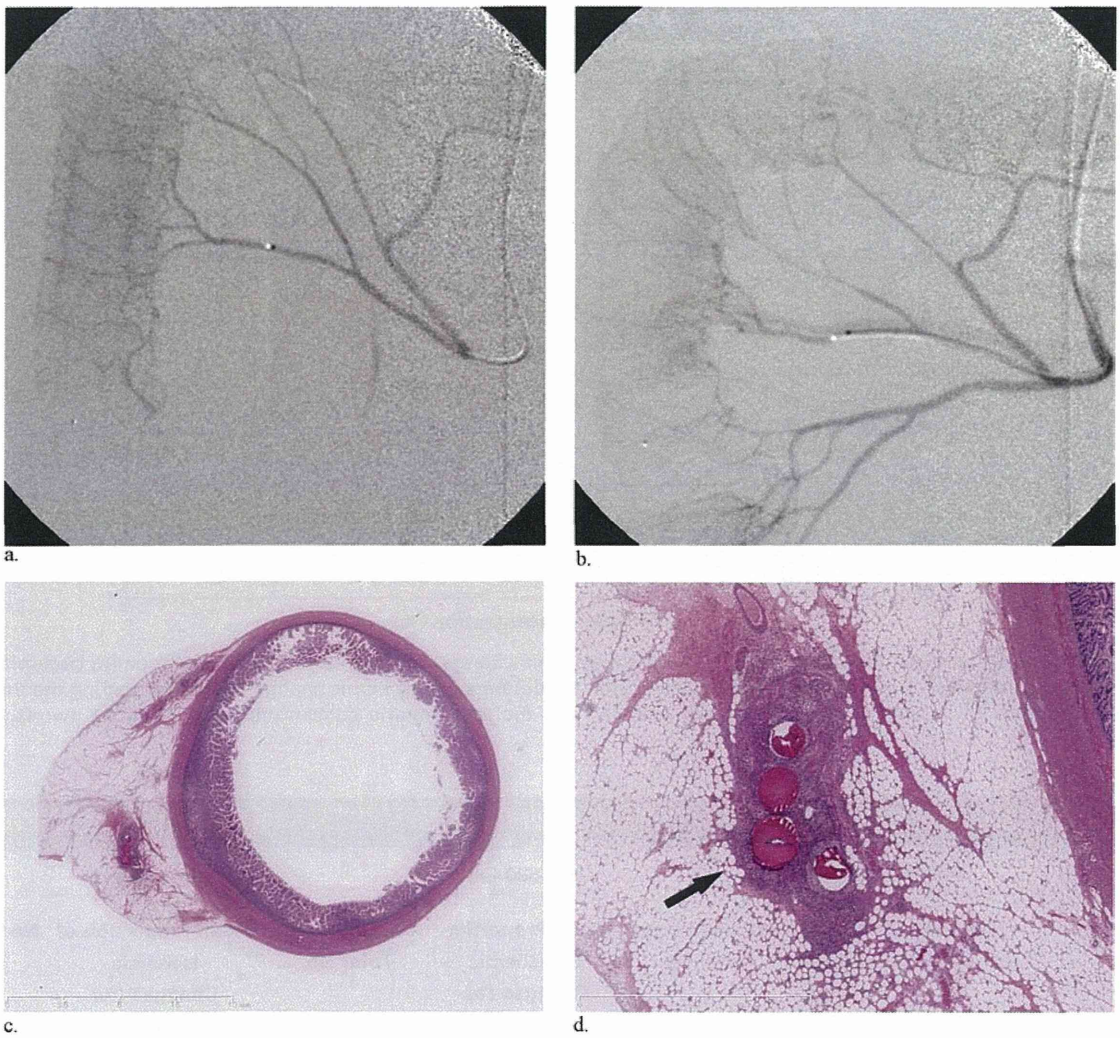

Figure 3. Selective angiogram of the peripheral branch of the superior mesenteric artery was obtained using a microcatheter. Before embolization, arcade, vasa recta, and mucosal blush are opacified **(a)**. After embolization with 500–700 μm microspheres (volume concentration 1.25%), only the vasa recta are occluded, whereas the arcade remains patent **(b)**. In the histologic axial-cut specimen (hematoxylin-eosin stain), no ischemic change is observed in the intestinal wall **(c)**. Four microspheres are seen in the mesentery (arrow) surrounded with mild infiltration of lymphocytes **(d)**.

ischemic changes were more severe when NBCA and ethiodized oil reached beyond a line, drawn two thirds from the mesenteric border on the radiographic findings, owing to the possible occlusion of the collateral communications between the vasa recta and submucosal interconnections. Likewise, 100–300 μm and 300–500 μm microspheres caused more severe ischemic changes because of deep penetration into the submucosal layer. In contrast, 500–700 μm microspheres were mainly located in the mesentery and could avoid occluding the collateral communication. However, even with 500–700 μm microspheres, ischemic change was equally observed in group B among three sizes of microspheres. Embolization should be limited to the vasa recta by using a small volume of microspheres.

Our study has several limitations. First, the results of our experiments in dogs cannot be translated directly to humans because the patterns and the diameters of the mesenteric vasculature of humans and dogs differ (19). Second, the long-term effects of embolization could not be evaluated because the animals were sacrificed 48 hours after embolization. However, 48 hours was thought to be sufficient time to cause acute ischemic changes at microscopic examination because ischemic changes were observed 24 hours after embolization in past studies (17,20). Third, only the small bowel was examined in the present study. The small intestine has a potentially better collateral blood supply than the colon (19). The effect on colonic embolization should be evaluated as well. Fourth, it is unclear if our results using Embospheres are consistent with effects of other microspheres with different properties and behavior (21,22). Fifth, the reviewers of the angiographic findings were from our team, and this could be considered a bias.

In conclusion, embolization limited to the vasa recta with the use of 500–700 μm microspheres was suitable

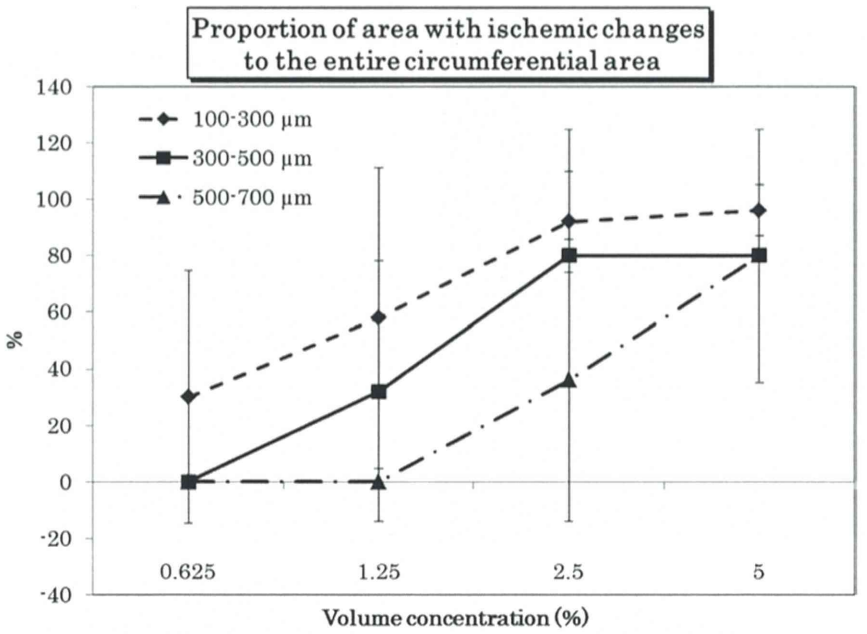

Figure 4. Relationship between the proportion of area with ischemic changes in the mucosal layer to the entire circumferential area and volume concentration of microspheres. There was a significant difference in ischemic changes when comparing the three different sizes of microspheres ($P = .004$, two-factor factorial ANOVA) and the four volume concentrations ($P < .0001$, two-factor factorial ANOVA).

Table 2. Percentage of Mean Proportion of Ischemic Changes in Mucosal Layer

	100–300 μm		300–500 μm		500–700 μm	
	Mean Proportion of Ischemic Changes (%)	No. Segments/ Total No.	Mean Proportion of Ischemic Changes (%)	No. Segments/ Total No.	Mean Proportion of Ischemic Changes (%)	No. Segments/ Total No.
Group A	60	15/20	30	12/20	0	12/20
Group B	90	5/20	75	8/20	83	8/20
P value (Mann-Whitney)	.29		.0502		.0001	

for mesenteric artery embolization. The range of ischemic changes of the intestinal wall correlated with angiographic findings.

ACKNOWLEDGMENT

This study was supported by JSPS KAKENHI Grant Number 23591819. We thank Kaishu Tanaka, MD, Yusuke Ono, MD, and Hiroki Higashihara, MD, PhD, of the Department of Diagnostic and Interventional Radiology of Osaka University Graduate School of Medicine for technical support.

REFERENCES

1. Weldon DT, Burke SJ, Sun S, Mimura H, Golzarian J. Interventional management of lower gastrointestinal bleeding. Eur Radiol 2008; 18: 857–867.
2. Millward SF. ACR Appropriateness Criteria on treatment of acute non-variceal gastrointestinal tract bleeding. J Am Coll Radiol 2008; 5:550–554.
3. Darcy M. Vascular embolotherapy. In: Golzarian J, Sun S, Sharafuddin M, editors. Embolization for Lower GI Bleeding. Heidelberg: Springer; 2006. p. 73–84.
4. Evangelista PT, Hallisey MJ. Transcatheter embolization for acute lower gastrointestinal hemorrhage. J Vasc Interv Radiol 2000; 11:601–606.
5. Kuo WT, Lee DE, Saad WE, Patel N, Sahler LG, Waldman DL. Superselective microcoil embolization for the treatment of lower gastrointestinal hemorrhage. J Vasc Interv Radiol 2003; 14:1503–1509.
6. Laurent A, Beaujeux R, Wassef M, Rufenacht D, Boschetti E, Merland JJ. Trisacryl gelatin microspheres for therapeutic embolization, I: development and in vitro evaluation. AJNR Am J Neuroradiol 1996; 17:533–540.
7. Laurent A. Microspheres and nonspherical particles for embolization. Tech Vasc Interv Radiol 2007; 10:248–256.
8. Siskin GP, Dowling K, Virmani R, Jones R, Todd D. Pathologic evaluation of a spherical polyvinyl alcohol embolic agent in a porcine renal model. J Vasc Interv Radiol 2003; 14:89–98.
9. Andrews RT, Binkert CA. Relative rates of blood flow reduction during transcatheter arterial embolization with tris-acryl gelatin microspheres or polyvinyl alcohol: quantitative comparison in a swine model. J Vasc Interv Radiol 2003; 14:1311–1316.
10. Pelage JP, Laurent A, Wassef M, et al. Uterine artery embolization in sheep: comparison of acute effects with polyvinyl alcohol particles and calibrated microspheres. Radiology 2002; 224:436–445.
11. Khankan AA, Osuga K, Hori S, Morii E, Murakami T, Nakamura H. Embolic effects of superabsorbent polymer microspheres in rabbit renal

model: comparison with tris-acryl gelatin microspheres and polyvinyl alcohol. Radiat Med 2003; 22:384–390.
12. Reuter SR, Chuang VP, Bree RL. Selective arterial embolization for control of massive upper gastrointestinal bleeding. Am J Roentgenol Radium Ther Nucl Med 1975; 125:119–126.
13. Maleux G, Roeflaer F, Heye S, et al. Long-term outcome of transcatheter embolotherapy for acute lower gastrointestinal hemorrhage. Am J Gastroenterol 2009; 104:2042–2046.
14. Kusano S, Murata K, Ohuchi H, Motohashi O, Atari H. Low-dose particulate polyvinylalcohol embolization in massive small artery intestinal hemorrhage. Experimental and clinical results. Invest Radiol 1987; 22: 388–392.
15. Derdeyn CP, Graves VB, Salamat MS, Rappe A. Collagen-coated acrylic microspheres for embolotherapy: in vivo and in vitro characteristics. AJNR Am J Neuroradiol 1997; 18:647–653.
16. Laurent A, Wassef M, Saint Maurice JP, et al. Arterial distribution of calibrated tris-acryl gelatin and polyvinyl alcohol microspheres in a sheep kidney model. Invest Radiol 2006; 41:8–14.
17. Jae HJ, Chung JW, Kim HC, et al. Experimental study on acute ischemic small bowel changes induced by superselective embolization of superior mesenteric artery branches with N-butyl cyanoacrylate. J Vasc Interv Radiol 2008; 19:755–763.
18. Ikoma A, Kawai N, Sato M, et al. Ischemic effects of transcatheter arterial embolization with N-butyl cyanoacrylate-lipiodol on the colon in a Swine model. Cardiovasc Intervent Radiol 2010; 33:1009–1015.
19. Ross JA. Vascular patterns of small and large intestine compared. Br J Surg 1952; 39:330–333.
20. Han YM, Lee JM, Jin KY, Lee SY, Kim CS. Embolization of superior mesenteric artery branches in dogs. Ischemic bowel changes depend on location of vessel occlusion and embolic materials. Invest Radiol 1999; 34:629–635.
21. Hidaka K, Moine L, Collin G, et al. Elasticity and viscoelasticity of embolization microspheres. J Mech Behav Biomed Mater 2011; 4: 2161–2167.
22. Stampfl S, Bellemann N, Stampfl U, et al. Arterial distribution characteristics of Embozene particles and comparison with other spherical embolic agents in the porcine acute embolization model. J Vasc Interv Radiol 2009; 20:1597–1607.

INVITED COMMENTARY

Particle Embolization: Factors Affecting Arterial Distribution

Jafar Golzarian, MD, and Lihui Weng, PhD

ABBREVIATION

LGI = lower gastrointestinal

Embolization of lower gastrointestinal (LGI) bleeding was first described in 1974 (1). With improvements in microcatheter technology and embolic agents resulting in better outcomes, embolization is now part of the treatment algorithm for patients with LGI bleeding. The most popular embolic agents used for LGI bleeding are microcoils because of their controlled deployment and good clinical outcome (2). Embolic particles or liquid agents can be used in cases in which reaching the bleeding vessel is technically challenging (3,4). For LGI bleeding, both the arterial distribution and the level of occlusion of particles are critical because nontarget embolization of the normal bowel can result in ischemic damage. Factors that should be considered when using particles for embolization include type, size, compressibility, aggregation, and flow dynamics.

From the Department of Radiology, University of Minnesota, 420 Delaware Street SE, Mayo B228, CMC 292, Minneapolis, MN 55414. Received August 18, 2014; accepted August 20, 2014. Address correspondence to J.G.; E-mail: jafar@umn.edu

J Vasc Interv Radiol 2014; 25:1773–1774

http://dx.doi.org/10.1016/j.jvir.2014.08.022

Different types of particles include spherical microspheres, nonspherical particles, and sterile sponges. Each type has unique occlusion characteristics (5). Using particles in very small sizes for LGI bleeding can lead to a high rate of infarction because smaller particles penetrate more distally (6,7). In their study on embolization of the small bowel using microspheres, Kishimoto et al (7) report that 100–300 μm microspheres (Embospheres; Merit Medical Systems, South Jordan, Utah) blocked vessels more distally than 500–700 μm microspheres limited to vasa recta and caused more ischemic damage to the mucosal layer. According to Kusao et al (6), to reduce the risk of ischemic lesions to the bowel, the particle size should not be < 300–500 μm. These authors used polyvinyl alcohol. Size selection also depends on the type of the embolic particles. When using spherical particles for embolization, a larger size is needed than when using nonspherical particles such as polyvinyl alcohol because of their compressibility characteristics.

Microsphere compressibility affects the level of vessel occlusion (5–7). Particle deformation allows improved injectability through the microcatheter and less clogging than occurs with nonspherical particles (8,9). This deformation can occur at the time of preparation, in the syringe, during the transition through the catheter, and inside the

Role of pyruvate kinase M2 in transcriptional regulation leading to epithelial–mesenchymal transition

Atsushi Hamabe[a,b,1], Masamitsu Konno[b,1], Nobuhiro Tanuma[c], Hiroshi Shima[c], Kenta Tsunekuni[a,d,e], Koichi Kawamoto[a,b], Naohiro Nishida[b], Jun Koseki[e], Koshi Mimori[f], Noriko Gotoh[g], Hirofumi Yamamoto[a], Yuichiro Doki[a,b,e], Masaki Mori[a,b,e,2], and Hideshi Ishii[b,e,2]

Departments of [a]Gastrointestinal Surgery and [b]Frontier Science for Cancer and Chemotherapy, Graduate School of Medicine, Osaka University, Osaka 565-0871, Japan; [c]Division of Cancer Chemotherapy, Miyagi Cancer Center Research Institute, Sendai 981-1293, Japan; [d]Taiho Pharmaceutical Co., Ltd., Chiyoda-ku, Tokyo 101-0054, Japan; [e]Department of Cancer Profiling Discovery, Graduate School of Medicine, Osaka University, Osaka 565-0871, Japan; [f]Department of Surgery, Kyushu University Beppu Hospital, Beppu 874-0838, Japan; and [g]Division of Cancer Cell Biology, Cancer Research Institute of Kanazawa University, Kanazawa 920-1192, Japan

Edited by Carlo M. Croce, The Ohio State University, Columbus, OH, and approved September 25, 2014 (received for review May 2, 2014)

Pyruvate kinase M2 (PKM2) is an alternatively spliced variant of the pyruvate kinase gene that is preferentially expressed during embryonic development and in cancer cells. PKM2 alters the final rate-limiting step of glycolysis, resulting in the cancer-specific Warburg effect (also referred to as aerobic glycolysis). Although previous reports suggest that PKM2 functions in nonmetabolic transcriptional regulation, its significance in cancer biology remains elusive. Here we report that stimulation of epithelial–mesenchymal transition (EMT) results in the nuclear translocation of PKM2 in colon cancer cells, which is pivotal in promoting EMT. Immunoprecipitation and LC-electrospray ionized TOF MS analyses revealed that EMT stimulation causes direct interaction of PKM2 in the nucleus with TGF-β–induced factor homeobox 2 (TGIF2), a transcriptional cofactor repressor of TGF-β signaling. The binding of PKM2 with TGIF2 recruits histone deacetylase 3 to the E-cadherin promoter sequence, with subsequent deacetylation of histone H3 and suppression of E-cadherin transcription. This previously unidentified finding of the molecular interaction of PKM2 in the nucleus sheds light on the significance of PKM2 expression in cancer cells.

pyruvate kinase M2 | epithelial–mesenchymal transition | colorectal cancer | invasion | transforming growth factor-β–induced factor homeobox 2

Colorectal cancer (CRC) is the second most common cancer in the world, with more than 1.2 million new cases and about 600,000 deaths annually (1). Cancerous cells exploit a cancer-specific glycolytic system known as the Warburg effect (also referred to as aerobic glycolysis), which involves rapid glucose uptake and preferential conversion to lactate, despite an abundance of oxygen (2, 3). The precise mechanism underpinning aerobic glycolysis was unclear for a long time. However, in 2008, pyruvate kinase M2 (PKM2) gained attention when its expression was shown to be required for the maintenance of aerobic glycolysis (4). PKM2 is an alternatively spliced variant of the PKM gene that regulates the final rate-limiting step of glycolysis. PKM2 is expressed during embryonic development, but it is generally not expressed in most adult tissues. However, its counterpart, PKM1, is exclusively expressed in adult tissues. PKM2 has been shown to be reactivated in tumor development (5, 6). In cancer cells, PKM2 expression allows the diversion of glycolytic flux into the pentose phosphate pathway associated with attenuated pyruvate kinase activity, thereby meeting the biosynthetic demands for rapid proliferation (3).

Investigations about the nuclear function of PKM2 arose after elucidation of the PKM2 metabolic function. It was identified that in cancer cells, PKM2 can translocate into the nucleus and function as a transcriptional cofactor in response to several extracellular signals, including EGF and hypoxia, subsequently activating CYCLIN D1, C-MYC, or hypoxia-inducible factor 1α (HIF-1α) (7, 8). Particularly in the hypoxic condition, PKM2 interacts with HIF-1α and participates in a positive feedback loop, thereby enhancing HIF-1α transactivation and reprogramming glucose metabolism by regulating the expression of glycolysis-associated enzymes (8). This finding suggested that the PKM2 nuclear function may operate upstream of metabolic regulation and that the resultant metabolic reprogramming and oncogene activation by PKM2 work cooperatively to promote cancer cell proliferation and tumor growth.

In addition to proliferation maintenance and growth suppression prevention, invasion and metastasis have also been targeted as hallmarks of cancer (9). In the invasion process, cancer cells acquire the ability to dissociate from the bulk of the tumor and to migrate into the surrounding stroma, which is regulated by epithelial–mesenchymal transition (EMT) (9, 10). During EMT, cancer cells lose their cell-to-cell contacts by

Significance

Our study shows that pyruvate kinase M2 (PKM2), an alternatively spliced variant of the pyruvate kinase gene, mediates epithelial–mesenchymal transition (EMT), which is critical for cancer cells to acquire invasive potential. Our study demonstrates that EMT stimulates nuclear translocation of PKM2 and decreases epithelial cadherin transcription (a requirement for EMT induction). Our results also demonstrate that PKM2 interacts with the transcriptional factor TGF-β–induced factor homeobox 2, which induces the deacetylation of histone H3, resulting in repressed E-cadherin expression. The precise understanding of nuclear PKM2 function suggests the potential for a model preventing cancer metastasis.

Author contributions: A.H., M.K., K.T., K.K., N.N., J.K., K.M., N.G., H.Y., Y.D., M.M., and H.I. designed research; A.H., M.K., and H.I. performed research; A.H., M.K., N.T., H.S., and H.I. contributed new reagents/analytic tools; A.H., M.K., J.K., N.G., M.M., and H.I. analyzed data; and A.H., M.K., N.T., H.S., K.T., K.K., N.N., J.K., K.M., N.G., M.M., and H.I. wrote the paper.

Conflict of interest statement: This work was supported in part by a Grant-in-Aid for Scientific Research from the Ministry of Education, Culture, Sports, Science, and Technology; a Grant-in-Aid from the Third Comprehensive 10-year Strategy for Cancer Control, Ministry of Health, Labor, and Welfare; a grant from the Kobayashi Cancer Research Foundation; a grant from the Princess Takamatsu Cancer Research Fund, Japan; a grant from the National Institute of Biomedical Innovation; and a grant from the Osaka University Drug Discovery Funds. A.H. is a research fellow of the Japan Society for the Promotion of Science. Partial support was received from Taiho Pharmaceutical Co., Ltd. (to J.K., M.M., and H.I.), Chugai Co., Ltd., Yakult Honsha Co., Ltd., Merck Co., Ltd., Takeda Science Foundation, and Takeda Medical Research Foundation (to M.K., N.N., M.M., and H.I.) through institutional endowments.

This article is a PNAS Direct Submission.

[1]A.H. and M.K. contributed equally to this work.

[2]To whom correspondence may be addressed. Email: mmori@gesurg.med.osaka-u.ac.jp or hishii@gesurg.med.osaka-u.ac.jp.

This article contains supporting information online at www.pnas.org/lookup/suppl/doi:10.1073/pnas.1407717111/-/DCSupplemental.